Original article

Differentiation of pituitary macroadenoma and craniopharyngioma in adult Patients: MRI findings

Panupong Radchauppanone,[1] Kanokporn Oranratanachai,[2] Salita Angkurawaranon,[2] Kittisak Unsrisong,[2] and Songkiet Suwansirikul[3]

[1]Deparment of Radiology, Chiangrai Prachanukroh Hospital, [2]Department of Radiology, [3]Department of Pathology, Faculty of Medicine, Chiang Mai University

Objective To compare the MRI findings between pituitary macroadenoma and craniopharyngioma.

Methods This retrospective study was conducted at our university Hospital. Patient data between January 2006 to June 2014 were reviewed. Pathological proof of pituitary macroadenoma 61 patients and other 10 patients of craniopharyngioma were included in the study. The patient data were categorized into gender and age. MRI findings analysed the tumor size, shape, component, adjacent brain edema, cavernous sinus invasion, sellar widening, presence of posterior T1-weighted bright spot, presence of normal pituitary gland, signal intensity of solid/cystic components on T1 and T2-weighted images and pattern of enhancement.

Results A snowman or ovoid shape with solid component, presence of sellar widening and posterior T1 bright spot were suggestive of pituitary macroadenoma ($p<0.05$). A lobulated shape with cystic component, presence of adjacent brain edema, epicenter of the tumor in suprasellar region which could be separable from the normal pituitary gland and presence of rim enhancement were suggestive of craniopharyngioma ($p<0.05$).

Conclusion MRI findings were helpful to distinguish between pituitary macroadenoma and craniopharyngioma by using tumor shape, component, sellar widening, presence of posterior T1 bright spot, adjacent brain edema, epicenter of the tumor in suprasellar region which could be separable from the normal pituitary gland and presence of rim enhancement. **Chiang Mai Medical Journal 2016;55(3):115-24.**

Keywords: MRI findings, pituitary macroadenoma, craniopharyngioma

Introduction

When the adult patient had sellar mass, the differential diagnosis usually included pituitary adenoma and craniopharyngioma[1-8]. Pituitary adenomas are benign neoplasm of pituicytes arising from adenohypophysis and account for 10-15% of all intracranial neoplasms[1]. Craniopharyngiomas arise from squamous epithelial cell remnants of Rathke's pouch and account for 1.2-4% of all intracranial tumors[1]. These tumors locate in sellar and suprasellar regions. When pituitary adenomas are larger than 10 mm, they are called pituitary macroadenoma.

Address correspondence to: Salita Angkurawaranon, M.D., Department of Radiology, Faculty of Medicine, Chiang Mai University,Chiang Mai, 50200, Thailand, E-mail: nook147@gmail.com
Received: December 15, 2016, **Accepted:** April 5, 2017.

Pituitary macroadenoma and craniopharyngioma patients usually have overlapping symptoms from local mass effect to adjacent optic pathway causing minimal visual field defect to blindness, hormonal disturbance and headache[9]. The optimal treatments of pituitary macroadenoma and craniopharyngioma are different. Correct diagnosis is important to choose proper treatment for each patient from medical treatment to surgery removal[10]. The transphenoidal route is the dominant surgical approach for pituitary macroadenoma[10-12]. On the other hand, patients with craniopharyngioma are traditionally treated with gross total section via craniotomy, and post-operative radiation should perform if the patient got subtotal resection[13,14].

The magnetic resonance imaging is an important modality which is less invasive to the patient and can provide good information for diagnosis of sellar mass[9]. Various characteristic imaging features of pituitary adenoma and craniopharyngioma have been described. Pituitary macroadenomas are typically isointense to gray matter on T1-weighted image, variable on T2-weighted image, and show heterogeneous or homogeneous enhancement in post contrast study[1,2]. They usually expand sellar turcica[4,6-8]. Pituitary macroadenomas can extend superiorly to supra-sellar region causing lobulated margin, snowman or figure of eight configulation from diaphragma sellae indentation[2,4,8].

Craniopharyngiomas have a bimodal age distribution, peak in children age 5-10 years and smaller peak in sixth decade of life. Craniopharyngioma can be classified as adamantinomatous and squamous papillary types base on histopathology[1,13,15]. The adamantinomatous types are predominantly cystic or mixed solid-cystic lobulated tumor, containing calcification. The cysts may also show signal isointensity to CSF or hyperintense on T1- and T2- weighted images due to high protein content or methemoglobin[4,5,7,8,15]. The squamous papillary types of craniopharyngioma are more common in adult. They are more solid without calcification as compared with classic adamantinomatous and usually have spherical shape rather than lobulated shape[7,15]. However there are still some overlapping findings between these tumors. This study plans to evaluate in more details the radiological findings to further characterize these diseases. The objective of this study is to compare MRI appearance of pituitary macroadenoma and craniopharyngioma for differentiation and diagnosis.

Materials and methods

Patients

This study was approved by the institutional review board and the informed consent was waived because of retrospective clinical study. A computerized search of our University's pathology database from January 2006 to June 2014 revealed that 204 patients were diagnosed with pituitary adenoma and 47 patients were diagnosed with craniopharyngioma. We included patients who had initial preoperative MRI brain at our hospital and pathological proof of pituitary adenoma and craniopharyngioma. 143 patients pituitary adenoma and 37 patients with craniopharyngioma were excluded from the study due to no pre-operative MRI, incomplete MR imaging, pediatric patients (younger than 15 years old) and pituitary microadenoma. Finally, 61 patients of pituitary macroadenoma and 10 patients of craniopharyngioma were included in this study.

MRI technique

All patients were performed brain MRI by using 1.5 T MRI machine (Signa Excite HDxt and Signa Excite HD with software version 12X and 16X, GE healthcare) and using 0.2 ml/kg (0.5 mmol/mL) of gadopentetated-imeglumine (Magnevist®) or gadoteric acid (DOTAREM®).

The MRI of each patient was performed with standard head coil in at least 6 sequences including axial FLAIR, Sagittal T1-weighted, Coronal T1-weighted, Coronal T2-weighted, post contrast sagittal and coronal T1-weighted.

MRI evaluation

All MR images were reviewed on a picture archiving and communication system (PACS) and using Synapse version 4.1 workstation. Two neuroradiologists evaluated MRI findings and consensus for each parameter. The neuroradiologists analyzed images with blind the patient's pathology for preventing bias.

Tumor size, shape, component, adjacent brain edema, cavernous sinus invasion, sellar widening, presence of posterior T1-weighted bright spot, presence of normal pituitary gland, signal of solid/cystic components on T1 and T2-weighted signals of solid or cystic components

on T1WI and T2WI and pattern of enhancement were evaluated.

Tumor size was defined as the largest antero-posterior (AP), transverse and vertical diameter and the tumor volume was calculated by formula; 0.5 x AP x transverse x vertical diameter. The tumor shapes were classified as ovoid, snowman and lobulated. A snowman shape was defined as a figure of eight-like appearance and a lobulated shape was applied if the tumor showed more than two lobes.

The components of the tumor were classified as; solid component was defined as more than 75% of tumor has solid component, cystic component was defined as more than 75% of tumor has cystic component and the other were classified as mix solid cystic component.

The adjacent brain edema was defined as presence of perilesional FLAIR hyperintense area. Cavernous sinus invasion was defined as presence of abnormal tissue between the lateral wall of the cavernous sinus and carotid artery[16]. Sellar widening was defined as the largest AP diameter is more than 16 mm and vertical diameter is more than 12 mm (The normal size of sella turcica ranges from 4 to 12 mm for the vertical dimension and 5 to 16 mm for the AP dimension)[17]. The presence of posterior T1-weighted bright spot was evaluated in sagittal non-contrast T1-weighted images. The term of normal pituitary gland was used if the pituitary gland can be separated from the tumor. The T1 and T2 signal intensities of solid component were defined into 4 types; hyperintense, isointense, hypointense and mixed signal intensities by comparison with the gray matter signal. The honeycomb appearance was defined as cluster of small T2 hyperintense foci within the solid component. The patterns of enhancing solid components were classified into homogeneous and heterogeneous enhancement. The T1 and T2 signal intensities of cystic component were defined as 4 type; hyperintense, isointense, hypointense and mixed signal intensities. Presence of rim enhancement was defined as enhancement of the peripheral part of the cystic portion is more than enhancing solid part enhancement. The presence of fluid-fluid level in all sequences was evaluated.

Statistical analysis

The two groups were compared by using the Student t-test for continuous data (age and tumor size). Results were given as mean±standard deviations. Chi-square test was used for categorical data (tumor shape, component, adjacent brain edema, cavernous sinus invasion, sellar widening, present of posterior T1-weighted bright spot, present of the normal gland, T1 and T2-weighted signals of solid or cystic components and pattern of enhancement). If the data were less than 5 in the group, Fisher's exact test was used.

Statistical analyses were performed by using software SPSS, version 17.0 (SPSS, Chicago, Ill). A *p* value of less than 0.05 was considered to indicate a statistically significant difference.

Results

General data

The study included 71 patients with pathological proof, which 61 patients revealed pituitary macroadenoma and 10 patients revealed craniopharyngioma. They were 39 male patients (33 of pituitary macroadenoma, 6 of craniopharyngioma) and 32 female patients (28 of pituitary macroadenoma, 4 of cranio-pharyngioma). The mean age of pituitary macroadenoma group was 47.18 years; range between 18-75 years. The mean age of cranio-pharyngioma group was younger than the group of pituitary macroadenoma, which was 33.8 years; ranges between 15 to 63 years. However, there was no statistically significant difference between these two groups (p= 0.056).

In 10 craniopharyngioma patients, there were 7 adamantinomatous and 3 squamous-papillary subtypes. The mean age of adamantinomatous subtype was less than squamous-papillary subtype, which revealed 30.29 years and 42.00 years, respectively. However, there was no statistically significant difference between these two groups (p=0.402).

MRI findings

The MRI findings of the pituitary macroadenoma and craniopharyngioma were summarized in Table 1. In the term of shape, there was statistically significant difference between pituitary macroadenoma and craniopharyngioma (p=0.007). Pituitary macroadenoma exhibited the diversity in shape, which could be lobulated (45.90%, 28 in 61 patient), snowman (31.15%, 19 in 61 patients) (Figure 1), and ovoid (22.95%, 14 in 61 patients). On the other hand, craniopharyngiomas were likely to be lobulated shape (Figure 2A) (100%, 10 in 10 patients). Area of brain edema was seen in craniopharyngioma higher than pituitary macroade-

Table 1. Comparison of MRI finding of pituitary macroadenoma and craniopharyngioma

Imaging findings		Pathology		*p*-value
		Pituitary macroadenoma (n=61)	Craniopharyngioma (n=10)	
Shape	Ovoid	14 (22.95%)	0	0.007*
	Snowman	19 (31.15%)	0	
	Lobulated	28 (45.90%)	10 (100%)	
Adjacent brain edema		5 (8.20%)	4 (40%)	0.019*
Cavernous sinus invasion		6 (9.84%)	0	0.585
Sellar widening		49 (80.33%)	4 (40%)	0.014*
Presence of posterior T1 bright spot		47 (77.05%)	4 (40%)	0.025*
Normal pituitary gland separates from tumor		0	3 (30%)	0.002*
Component	Solid	38 (62.30%)	1 (10%)	0.000*
	Mix	20 (32.79%)	2 (20%)	
	Cystic	3 (4.91%)	7 (70%)	
Size (mean±SD in cm, volume cm^3)	AP	2.55±0.98	3.54±1.34	0.058
	Transverse	2.81±1.04	3.3±0.77	0.104
	Vertical	3.29±1.22	3.73±1.49	0.356
	Volume	16.09±18.97	30.41±30.47	0.134

* statistically significant difference ($p<0.05$)

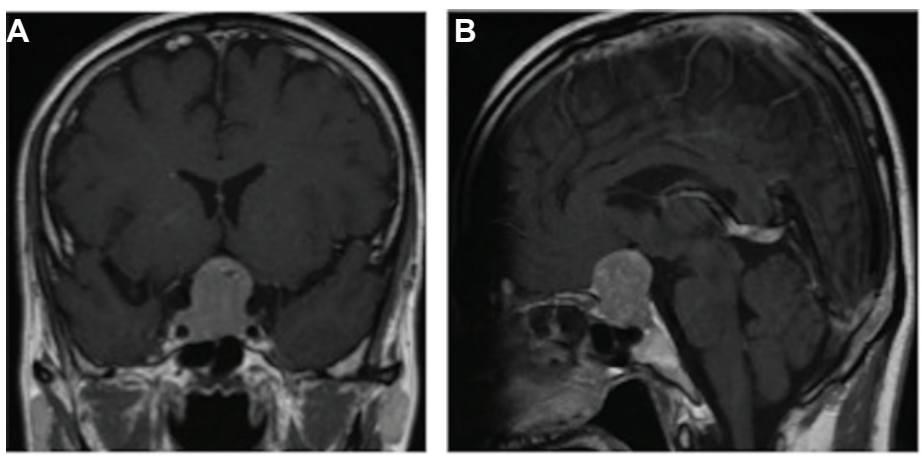

Figure 1. Post gadolinium coronal (A) and sagittal (B) T1-weighted images of a 52 years old man with pituitary macroadenoma show solid mass with snowman appearance and sellar widening.

noma (40% and 8.2%, respectively; p=0.019) (Figure 3). Pituitary macroadenomas had sellar widening and posterior T1 bright spot more than craniopharyngioma (p=0.014 and 0.025, respectively). Tumor originated in the suprasellar region and could be separated from the normal pituitary gland was found in 30% of craniopharyngioma(Figure 2B), but 0% of pituitary macroadenoma (p=0.002). Cavernous sinus invasion could be seen in pituitary macroadenoma (9.84%) but 0 % in craniopharyngioma. There is no significant different between both tumors (p=0.585). According to tumor component, there was statistically significant difference between pituitary macroadenoma and craniopharyngioma (p=0.000). The

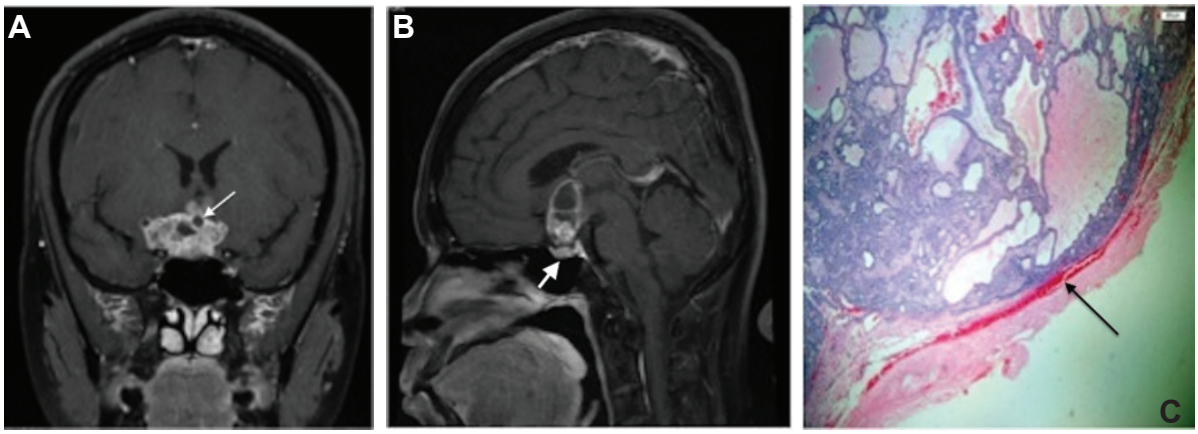

Figure 2. (A) Post contrast coronal T1-weighted image of a woman with craniopharyngioma shows a lobulated mix solid cystic lesion with rim enhancement of the cystic portion (arrow). (B) Sagittal T1 post contrast of a woman with craniopharyngioma shows a lobulated mix solid cystic lesion with rim enhancement of the cystic portion. Also noted tumor locates in suprasellar and can be separated from the normal pituitary gland (arrow). (C). Pathology (low power field) of patient A shows prominent vascular space in the cyst wall (arrow).

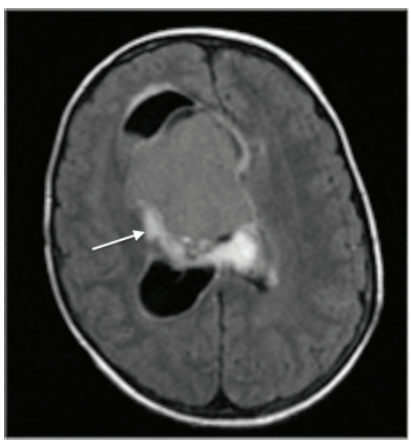

Figure 3. Axial FLAIR image of a woman with craniopharyngioma shows area of hyperintense perilesional brain edema.

pituitary macroadenomas were more likely to be solid mass (62.30% versus 10%), while craniopharyngiomas were more likely to be cystic mass (70% versus 4.91%). Nevertheless, there was no statistically significant difference in tumor size and volume between these two groups.

The signal intensities and MRI findings of solid part were evaluated in both groups of solid mass and mixed solid-cystic lesion (58 patients of pituitary macroadenoma and 3 patients of craniopharyngioma) and were summarized in Table 2. There was no significant difference between these tumors when evaluation with T1 and T2 signal intensities. Pituitary macroadenoma and craniopharyngioma were usually isointense T1 signal to the gray matter (89.66% and 66.67%, respectively) and they were usually hyperintense T2 signal to the gray matter (68.97% and 100%, respectively). Honeycomb appearance was shown in pituitary macroadenoma than craniopharyngioma (68.97% and 33.33%, respectively), but there was no statistically significant difference (p =0.248). Enhancement of the solid part in both kinds of tumors was heterogeneous (93.10% in pituitary macroadenoma and 100 % in craniopharyngioma; p=1.00).

The signal intensities and MRI findings of the cystic part were evaluated in both groups of solid mass and mixed solid-cystic lesion (23 patients of pituitary macroadenoma and 9 pa-

Table 2. Comparison solid parts of pituitary macroadenoma and craniopharyngioma

Imaging findings		Pathology		*p*-value
		Pituitary macroadenoma (n=58)	Craniopharyngioma (n=3)	
T1 signal of solid component	Hypointense	1 (1.72%)	1 (33.33%)	0.192
	Isointense	52 (89.66%)	2 (66.67%)	
	Hyperintense	3 (5.17%)	0	
	Mixed signals	2 (3.45%)	0	
T2 signal of solid component	Hypointense	6 (10.34%)	0	1.000
	Isointense	9 (15.52%)	0	
	Hyperintense	40 (68.97%)	3 (100%)	
	Mixed signals	3 (5.17%)	0	
Presence of honey combing appearance		40 (68.97%)	1 (33.33%)	0.248
Enhancement	Homogeneous	4 (6.90%)	0	1.000
	Heterogeneous	54 (93.10%)	3 (100%)	

Table 3. Comparison cystic parts of pituitary macroadenoma and craniopharyngioma

Imaging findings		Pathology		*p*-value
		Pituitary macroadenoma (n=23)	Craniopharyngioma (n=9)	
T1 signal of cysticcomponent	Hypointense	12 (52.17%)	6 (66.67%)	0.203
	Isointense	1 (4.35%)	0	
	Hyperintense	9 (39.13%)	1 (11.11%)	
	Mixed signals	1 (4.35%)	2 (22.22%)	
T2 signal of cystic component	Hypointense	0	1 (11.11%)	0.073
	Isointense	0	0	
	Hyperintense	23 (100%)	7 (77.78%)	
	Mixed signals	0	1 (11.11%)	
Presence of rim enhancement		0	7 (77.78%)	0.000*
Presence of fluid-fluid level		8 (34.78%)	0	0.149

* statistically significant difference ($p<0.05$)

tients of craniopharyngioma) and were summarized in Table 3. The cystic part of both tumors were usually hypointense in T1 weighted image (52.17% in pituitary macroadenoma and 66.67% in craniopharyngioma; $p=0.203$) and hyperintense in T2 weigthed image (100% in pituitary macroadenoma and 77.78% in craniopharyngioma; $p=0.073$). If there was rim enhance of the tumor (Figure 2A), It would be craniopharyngioma ($p=0.000$). Presence of fluid-fluid level could be seen in the pituitary macroadenoma which was 34.78% but none of the craniopharyngioma was shown (0%), there was no statistically significant difference ($p=0.149$)

Discussion

Pituitary adenomas represent 10-15% of all intracranial neoplasm and craniopharyngiomas account for 1.2-4% of all intracranial tumors. These tumors share the same locations in sellar and suprasellar regions, but the optimal treatments are different. Thus, the precised diagnosis is required.

More than 70% of patients with pituitary macroadenoma in this study were 30-60 years old and craniopharyngiomas showed bimodal age distribution (teenagers and adults) which are compatible with the previous literatures[1, 12]. There was no sex predilection in both tumors.

This study corresponded with the previous study by S.H. Choi in Korea[2] that pituitary macroadenomas usually have solid component with associated snowman shape while craniopharyngiomas usually have lobulated shape with cystic component. In addition, this study revealed that the ovoid shaped tumor with solid component was more common in pituitary macroadenoma as compared to the craniopharyngioma. Furthermore, this study revealed that when presence of sellar widening was suggestive of pituitary macroade-noma. This finding could possibly represent tumor origin itself in sellar region and slow growing nature of this tumor. In the meantime, craniopharyngioma, mostly for tumor origin, is located in the suprasellar region[18] about 78.5% and in the intrasellar/suprasellar region about only 21.4% according to prior study[15]. The other present finding is posterior T1 bright spot which also was suggestive of pituitary macroadenoma. Because of different tumor origin between these tumors, most of pituitary macroadenoma arises from the anterior lobe of pituitary gland (adenohypophysis)[19] but craniopharyngioma originates from craniophayngeal duct and pars tuberalis which are located close to the pituitary stalk[20]. That is why this focused finding may be useful to differentiate pituitary macroadenoma from craniopharyngioma.

This study also revealed that 30% of craniopharyngiomas located in the suprasellar region and could be separated from normal pituitary gland in the sellar turcica. Area of adjacent brain edema was more common in craniopharyngioma which could be from direct compression of the mass. The more tumor enlarges, the more compression into adjacent brain parenchyma. There were 9 lesions in this study which had adjacent brain edema (mean tumor volume 40.00 cm^3±32.36) to compare with 62 lesions without adjacent brain edema (mean tumor volume 14.22 cm^3±16.59) (p=0.045). The signal intensities on T1WI and T2WI of the solid and cystic components between these two groups were not different.

Presence of rim enhancement is helpful for differentiation in mixed solid-cystic mass, which was shown approximately 77.78% in craniopharyngiomas while none of the in pituitary macroadenoma had this feature. The pathological review (Figure 2C) showed that craniopharyngiomas had prominent vascular space in the cystic wall which could result in rim enhancement after gadolinium administration. On the other hand, the cystic portion of pituitary macroadenomas could be the result from cystic degeneration and necrosis thus no enhancement after gadolinium injection was reasonable[21].

Hemorrhage in craniopharyngioma was rare[22,23]. On the contrary, pituitary adenoma with intratumoral haemorrhage was frequently appeared. Besides, 50% of the pituitary macroadenomas might contain cyst, hemorrhage or both of them[23]. Debris-fluid or fluid-fluid level was likely from intratumoral hemorrhage or cystic degeneration[21]. Only pituitary macroadenoma showed fluid-fluid level in this study (34.78% versus 0%, p=0.149). Furthermore, there was correlation between the findings of fluid-fluid level and haemorrhage in the pituitary macroadenoma which was proven by pathology.

In coronal T2-weighted image, the presence of honeycomb appearance was seen more often in the pituitary macroadenoma as compared to the craniopharyngioma (68.97% vs 33.33%, p=0.248). On coronal GRE T2*, some lesions with honeycomb appearance also showed dark signal intensities that represented intratumoral hemorrhage. Histopathological examination in one of pituitary macroadenoma with honey comb appearance showed diffuse hemorrhage in the tumor. Likewise in a prior study, honeycomb-like appearance with mixed high signal intensity on T2W in pituitary adenoma was also correlated with hemorrhage on histopathological examination[24]. However, it should be noted that dark signal lesions on GRE T2*image could be the result from haemorrhage, calcification, iron deposit, or melanin.

Invasion of cavernous sinus was rare in craniopharyngioma[8,25], but it was more common in pituitary macroadenoma (9.84% versus 0% in craniopharyngioma). However, there was no statistically significant, p= 0.585. The study from S.H. Choi[2] showed that both tumors

can extend beyond lateral wall of the cavernous ICA.

There were some limitations of this study. First, this study was retrospective review of imaging interpretations using consensus reading of two neuroradiologist without interobserver variability assessment. Second, we could not correlate all of the imaging findings with pathologic findings. Third, we included only pituitary macroadenoma and craniopharyngioma (common lesions in sellar and suprasellar), but other uncommon lesions in this region such as Rathke cleft cyst, meningiomas, glioma, germ cell tumor, aneurysms, metastates, and granulomatous disease were not included.

In conclusion, MRI findings such as shape of the tumor and its component are useful to differentiate between pituitary macroadenoma and craniopharyngioma. Presence of sellar widening and posterior T1 bright spot are frequently found in pituitary macroadenoma. On the other hand, area of adjacent brain edema, suprasellar origin with presence of normal pituitary gland and presence of rim enhancement are the features that suggestive of craniopharyngioma.

References

1. **Osborn AG**. Sellar neoplasm and tumor-like lesions. In: Osborn AG, editor. Osborn's Brain: Imaging, Pathology, and Anatomy. Salt Lake City, UT: Amirsys; 2012. p. 681-725.
2. **Choi SH, Kwon BJ, Na DG, Kim JH, Han MH, Chang KH**. Pituitary adenoma, craniopharyngioma, and Rathke cleft cyst involving both intrasellar and suprasellar regions: differentiation using MRI. Clin Radiol 2007;62:453-62.
3. **Sautner D, Saeger W, Ludecke DK.** Tumors of the sellar region mimicking pituitary adenomas. Exp Clin Endocrinol 1993;101:283-9.
4. **Connor SE, Penney CC.** MRI in the differential diagnosis of a sellar mass. Clin Radiol. 2003;58:20-31.
5. **Rao VJ, James RA, Mitra D.** Imaging characteristics of common suprasellar lesions with emphasis on MRI findings. Clin Radiol 2008;63:939-47.
6. **Rennert J, Doerfler A.** Imaging of sellar and parasellar lesions. Clinical Neurology and Neurosurgery 109:111-24.
7. **Kumar J, Kumar A, Sharma R, Vashisht S.** Magnetic resonance imaging of sellar and suprasellar pathology: a pictorial review. Curr Probl Diagn Radiol 2007;36:227-36.
8. **Donovan JL, Nesbit GM.** Distinction of masses involving the sella and suprasellar space: specificity of imaging features. American Journal of Roentgenology 1996;167:597-603.
9. **Famini P, Maya MM, Melmed S.** Pituitary magnetic resonance imaging for sellar and parasellar masses: ten-year experience in 2598 patients. J Clin Endocrinol Metab 2011;96:1633-41.
10. **Wilson CB.** Surgical management of pituitary tumors. J Clin Endocrinol Metab 1997;82:2381-5.
11. **Laws ER, Jane JA, Jr.** Neurosurgical approach to treating pituitary adenomas. Growth Horm IGF Res 2005;15 Suppl A:S36-41.
12. **Osborn AG.** Pituitary macroadenoma. In: Osborn AG, L.Salman K, Barkovich AJ, editors. Diagnostic imaging : brain. second ed. Salt Lake City, UT: Amirsys; 2010. p. II-2-26.
13. **Rees FH.** Craniopharyngioma. In: Osborn AG, L.Salman K, Barkovich AJ, editors. Diagnostic imaging : brain. Second ed. Salt Lake City, UT: Amirsys; 2010. p. II-2-34.
14. **Elliott RE, Jane JA, Jr., Wisoff JH.** Surgical management of craniopharyngiomas in children: meta-analysis and comparison of transcranial and transsphenoidal approaches. Neurosurgery. 2011;69:630-43; discussion 43.
15. **Sartoretti-Schefer S, Wichmann W, Aguzzi A, Valavanis A.** MR differentiation of adamantinous and squamous-papillary craniopharyngiomas. AJNR Am J Neuroradiol 1997;18:77-87.
16. **Symons SP, Montanera WJ, Aviv RI, Kucharczyk W.** The Sella Turcica and Parasellar Region. In: Atlas SW, editor. Magnetic Resonance Imaging of the Brain and Spine. Fourth ed. Philadelphia, PA: Lippincott Williams & Wilkins, a Wolters Kluwer business; 2009. p. 1142-3.
17. **Sathyanarayana HP, Kailasam V, Chitharanjan AB.** Sella turcica-Its importance in orthodontics and craniofacial morphology. Dental Research Journal. 2013;10:571-5.
18. **Symons SP, Montanera WJ, Aviv RI, Kucharczyk W.** The Sella Turcica and Parasellar Region. In: Atlas SW, editor. Magnetic Resonance Imaging of the Brain and Spine. Fourth ed. Philadelphia, PA: Lippincott Williams & Wilkins, a Wolters Kluwer business; 2009. p. 1145.
19. **Smith AB, Cha S.** Sellar and Juxtaselar Tumors. In: Naidich TP, Castillo M, Cha S, Smirniotopoulos JG, editors. Imaging of the Brain. Saunders; 2012. p. 728-53.
20. **Sartoretti-Schefer S, Wichmann W, Aguzzi A, Valavanis A.** MR differentiation of adamantinous and squamous-papillary craniopharyngiomas.

American Journal of Neuroradiology 1997;18:77-87.
21. **Symons SP, Montanera WJ, Aviv RI, Kucharczyk W.** The Sella Turcica and Parasellar Region. In: Atlas SW, editor. Magnetic Resonance Imaging of the Brain and Spine. Fourth ed. Philadelpia: Lippincott Williams & Wilkins, a Wolters Kluwer business; 2009. p. 1139-40.
22. **Chang CV, Nunes Vdos S, Felicio AC, Zanini MA, Cunha-Neto MB, de Castro AV.** Mixed germ cell tumor of the pituitary-hypothalamic region presenting as craniopharyngioma: case report and review of the literature. Arq Bras Endocrinol Metabol 2008;52:1501-4.
23. **Ishii K, Isono M, Hori S, Kinba Y, Mori T.** [A case of craniopharyngioma with intratumoral hemorrhage]. No Shinkei Geka. 1999;27:73-7.
24. **Tosaka M, Sato N, Hirato J, Fujimaki H, Yamaguchi R, Kohga H, et al.** Assessment of hemorrhage in pituitary macroadenoma by T2*-weighted gradient-echo MR imaging. AJNR Am J Neuroradiol 2007;28:2023-9.
25. **Buchfelder M, Schlaffer S.** Imaging of pituitary pathology. In: Fliers E, Korbonits M, Romijn JA, editors. Handbook of Clinical Neurology. Elsevier B.V.; 2014. p. 160.

การแยก pituitary macroadenoma และ craniophagyngioma ในผู้ป่วยผู้ใหญ่จากภาพเอกซเรย์คลื่นแม่เหล็กไฟฟ้า

ภาณุพงศ์ ราชอุปนันท์,[1] กนกพร โอฬารรัตนชัย,[2] สลิตา อังกุระวรานนท์,[2] กิตติศักดิ์ อุ่นศรีส่ง[2] และ ทรงเกียรติ สุวรรณศิริกุล[3]
[1]โรงพยาบาลเชียงรายประชานุเคราะห์, [2]ภาควิชารังสีวิทยา, [3]ภาควิชาพยาธิวิทยา คณะแพทยศาสตร์ มหาวิทยาลัยเชียงใหม่

วัตถุประสงค์ เพื่อเปรียบเทียบความแตกต่างของภาพเอกซเรย์คลื่นแม่เหล็กไฟฟ้าระหว่าง pituitary macroadenoma และ craniopharyngioma

วิธีการ เป็นการวิจัยแบบย้อนหลังจากภาพเอกซเรย์คลื่นแม่เหล็กไฟฟ้าระหว่างเดือนมกราคม พ.ศ. 2549 ถึงเดือนมิถุนายน พ.ศ. 2557 ผู้ป่วยที่มีผลพยาธิวิทยาเป็นpituitary macroadenomaจำนวน 61 ราย และ craniopharyngiomaจำนวน 10 ราย รวมรวมข้อมูลเกี่ยวกับผู้ป่วยเรื่อง เพศ อายุ ข้อมูลของก้อนเนื้องอก ได้แก่ ขนาด รูปร่าง องค์ประกอบของก้อน การมีสมองรอบข้างบวม การมีการกว้างขึ้นของกระดูกเซลล่า เทอร์ซิกา การรุกล้ำของก้อนเนื้องอกเข้าไปยังโพรงหลอดเลือดดำใต้ฐานสมอง การพบกลีบหลังของต่อมใต้สมอง การที่ต่อมใต้สมองสามารถแยกออกจากเนื้องอกได้ สัญญาณภาพที่ได้จากส่วนที่เป็นของแข็งและของเหลวของก้อนเนื้องอกและรูปแบบการ enhancement ของก้อนเนื้องอก

ผลการวิจัย ก้อนเนื้องอกที่มีรูปร่างแบบมนุษย์หิมะหรือรูปวงรี มีองค์ประกอบเป็นของแข็ง การมีการกว้างขึ้นของกระดูกเซลล่า เทอร์ซิกา และเห็นกลีบหลังของต่อมใต้สมองพบได้ใน pituitary macroadenomaแบบมีนัยสำคัญทางสถิติ ก้อนเนื้องอกรูปร่างแบบลอน ๆ องค์ประกอบเป็นถุงน้ำ การพบสมองรอบข้างบวม ศูนย์กลางของก้อนเนื้องอกอยู่เหนือเซลล่า เนื้องอกสามารถแยกออกจากต่อมใต้สมองได้และลักษณะ enhancement เป็นที่ขอบของก้อนพบได้ ใน craniopharyngioma แบบมีนัยสำคัญทางสถิติ

สรุปผลการวิจัย เอกซเรย์คลื่นแม่เหล็กไฟฟ้าช่วยในการแยกระหว่าง pituitary macroadenoma และ craniopharyngiomaโดยอาศัยรูปร่าง องค์ประกอบของก้อนเนื้องอก การมีการกว้างขึ้นของกระดูกเซลล่า เทอร์ซิกา การพบกลีบหลังของต่อมใต้สมอง ศูนย์กลางของเนื้องอกอยู่เหนือเซลล่า การที่สามารถแยกต่อมใต้สมองออกจากก้อนเนื้องอกได้ และการมี enhancement ที่ขอบของก้อน **เชียงใหม่เวชสาร 2559;55(3):115-24.**

คำสำคัญ: ภาพเอกซเรย์คลื่นแม่เหล็กไฟฟ้า, pituitary macroadenoma, craniopharyngioma